Biochemical and Biophysical Research Communications 421 (2012) 731–735

Contents lists available at SciVerse ScienceDirect

Biochemical and Biophysical Research Communications

journal homepage: www.elsevier.com/locate/ybbrc

A protein switch with tunable steepness reconstructed in *Escherichia coli* cells with eukaryotic signaling proteins

Masahiro Takahashi [a], Tatsuo Shibata [b], Toshio Yanagida [c], Yasushi Sako [a,*]

[a] Cellular Informatics Laboratory, RIKEN Advanced Science Institute, Wako, Saitama 351-0198, Japan
[b] Laboratory for Physical Biology, RIKEN Center for Developmental Biology, Kobe, Hyogo 650-0047, Japan
[c] Laboratories of Nano-Biosciences, Graduate School of Frontier Biosciences, Osaka University, Suita, Osaka 565-0871, Japan

ARTICLE INFO

Article history:
Received 11 April 2012
Available online 20 April 2012

Keywords:
Zeroth-order ultrasensitivity
MAPK cascade
Protein phosphorylation and dephosphorylation
Reconstruction

ABSTRACT

An important goal of synthetic biology is to construct reaction circuits with artificial responses by assembling modulated biological elements into living cells. While many such attempts have been based upon the cellular transcriptional apparatus, the use of the post-translational machinery remains relatively rare. Here we report the reconstruction in *Escherichia coli* of a protein-based artificial module based upon elements of a eukaryotic cell signaling pathway. The module shows a switch-like ultrasensitive response, using the opposing functions of a protein kinase and a phosphatase. The switch is acutely responsive to the kinase:phosphatase ratio, and can be modulated as a function of the expression level of the substrate. We can theoretically predict the response of this module and can control its steepness based on these predictions. Future work will demonstrate the potential of this controllable protein-based switch to be incorporated into artificial circuits.

1. Introduction

Gene-based circuits have been applied to recapitulate various complex functions in synthetic biology [1–5]. In the cell, however, the complex dynamics of cellular signal processing and biological responses are dependent not only upon gene function but also upon protein function, and protein-based signaling can be incorporated into synthetic biological circuits [6]. Indeed, rewiring of reaction pathways [7,8] and modulating the output of these pathways [9,10] have both been achieved by engineering of protein reactions in the context of cell signaling. These works attempted analyzes of the mechanism of cell signaling. We are interested in the application of protein reactions to assemble modules to be used in artificial biological circuits, and, here, aimed to construct a switch-like protein module.

The characteristic feature of a biological switch is an ultrasensitive response which could result from dynamics of opposing reactions, namely activation and inactivation [11]. Among opposing protein reactions, the regulation of phosphoproteins by kinases (phosphorylation) and phosphatases (dephosphorylation) is a well-known paradigm. Applying this paradigm to a switch-like module, the kinase:phosphatase ratio is the input and the phosphorylation level of the substrate is the output. In this context, the response of the switch can theoretically be predicted by applying Michaelis–Menten kinetics to each individual phosphorylation and dephosphorylation step [11].

The eukaryotic mitogen-activated protein kinase (MAPK) cascade mediates myriad cellular responses, including those involved in cell proliferation and differentiation [12,13]. We are interested in one of the reactions in MAPK cascade, the dual phosphorylation of extracellular signal-regulated kinase (ERK) as a candidate protein switch. Specific threonine and tyrosine residues of ERK are subject to tandem phosphorylation and dephosphorylation reactions catalyzed by MAPK/ERK kinase (MEK) [14,15] and MAP kinase phosphatase (MKP) [16], respectively (Fig. 1A). The dual phosphorylated ERK (ERKpp) is the active form of the protein.

We constructed an artificial switch-like module based on the response characteristics of ERKpp as a function of MEK and MKP activities. In order to make the switch independent of the host cell reactions, eukaryotic protein reactions were incorporated in the context of prokaryotic cells. In this system, important determinants of ultrasensitivity are (i) the two-step reaction (dual phosphorylation and dephosphorylation) and (ii) the saturation of Michaelis–Menten kinetics [11].

2. Materials and methods

2.1. Vector construction

The expression vector for ERK was based on pBAD (Invitrogen) (Fig. 1B, Supplementary Fig. 1A). A K54A mutation which abolishes

* Corresponding author. Fax: +81 48 462 4671.
E-mail address: sako@riken.jp (Y. Sako).

0006-291X/$ - see front matter © 2012 Elsevier Inc. All rights reserved.
http://dx.doi.org/10.1016/j.bbrc.2012.04.071

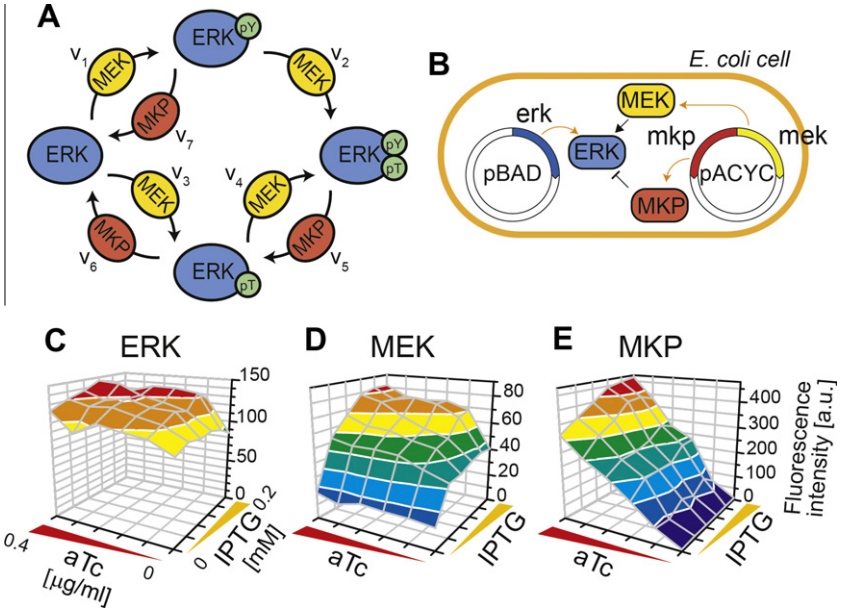

Fig. 1. Reconstruction of the ERK, MEK, and MKP system in *E. coli* cells. (A) Reaction diagram of ERK activation [26]. Two-step phosphorylation and dephosphorylation at T187 and Y189 of ERK are regulated by MEK and MKP, respectively. The dual-phosphorylated form (ERKpp) is the active form. (B) The reaction system of ERK phosphorylation was reconstructed in *E. coli* cells using expression vectors of Cerulean-ERK, and Venus-MEK and mCherry-MKP. (C–E) Expression levels of ERK, MEK, and MKP are controlled by changing the concentrations of arabinose, IPTG, and aTc, respectively, in the culture medium. Expression levels of the three proteins were measured in cell suspensions cultured for 24 h at the indicated concentrations of IPTG and aTc. The concentration of arabinose was constant (0.2%). Averages of 5 independent experiments are plotted.

the kinase activity of human ERK2 was introduced by fusion PCR [17]. The mutant ERK2 gene was fused to the 3′ end of Cerulean (a cyan fluorescent protein variant) gene [18] with a 9× Gly linker, and cloned into the restriction sites between *NcoI* (forward) and *SacI* (reverse) of pBAD. The Cerulean-ERK2 was under the regulation of the *araBAD* promoter [19].

A gene encoding a constitutively active form of MEK1 (S218/222E Δ32–51) [20] was constructed from pFC-MEK1 (STRATAGENE), to which were added restriction sites for *Sal*I (forward) and *Xba*I (reverse) at both ends. The MKP3 gene [21] was obtained from GenBank, and restriction sites for *Xho*I (forward) and *Xba*I (reverse) were added to the both ends. The Venus (encoding a yellow fluorescent protein variant) [22] and mCherry (encoding a red fluorescent protein variant) genes [23] were fused with the Shine–Dalgarno sequence [24] at the 5′ end and 8× Gly linker at the 3′ end, then a restriction site for *Bgl*II was added to the forward end, and *Sal*I or *Xho*I was added to the reverse end of Venus or mCherry, respectively. The expression vector for Venus-MEK1 and mCherry-MKP3 was based on pACYC184 (BioLabs) (Supplementary Fig. 1B). The *lac* and *tet* promoter [25] were synthesized using artificial primers by fusion PCR, and the T1T2 terminator was cloned from *Escherichia coli* genome. Each promoter was fused with the T1T2 terminator by PCR and inserted between the *Eag*I and *Ase*I sites of pACYC184. The Venus, MEK1, mCherry, and MKP3 genes were inserted between each promoter and the terminator using restriction sites for *Bgl*II and *Sal*I (Venus), *Sal*I and *Xba*I/*Spe*I (MEK1), *Bam*HI/*Bgl*II and *Xho*I (mCherry), and *Xho*I and *Xba*I (MKP3), respectively. The Venus-MEK1 and mCherry-MKP3 genes were under the regulation of *lac* and *tet* promoter, respectively.

2.2. Cell culture

E. coli DH5αZ1 [25] co-transformed with the two expression plasmids was cultured in 5 ml LB medium with 50 μg/ml kanamycin and 25 μg/ml chloramphenicol for 24 h at 37 °C with shaking. The culture medium contained 0.2 or 0.066% arabinose (Wako) for high and low expressions of ERK, respectively, 0–0.133 mM IPTG (Wako) for MEK, and 0–0.311 μg/ml aTc (Clontech) for MKP. Cell growth was measured by at OD_{600} after 20-fold dilution with LB medium using a U-3000 spectrophotometer (Hitachi).

2.3. Measurement of protein expression levels

The relative expression levels of ERK, MEK and MKP were determined from the emission intensity of fluorescent proteins fused to each protein. Cultured cells were collected by centrifugation and suspended in water. The emission intensities of Cerulean, Venus, and mCherry were measured at excitation/emission wavelengths 433/470–490 nm, 488/520–540 nm, and 587/600–620 nm, respectively, using a RF-5300PC fluorometer (Shimadzu) and normalized by the cell densities determined from OD_{600}. Autofluorescence signals of cells were determined using untransformed *E. coli* cells and subtracted from the signals of each sample.

2.4. Measurements of protein phosphorylations

Protein phosphorylation was measured by Western blotting. Standard SDS–PAGE and transfer procedures were used. Primary antibodies used were anti-phospho-p44/42 MAPK (E10) (Cell Signaling Technology) and anti-phosphotyrosine (PY20) (Upstate). Staining was carried out using VECTASTAIN ABC System (Vector Laboratories). The staining intensities were quantified using the plug-in of gel analysis in ImageJ software. The intensities were normalized against number of cells determined from OD_{600}.

2.5. Data fittings

The plots of ERKpp/ERK versus MEK/MKP were fitted using Origin software (OriginLab). Four independent experiments were carried out for each arabinose concentration. The results of four experiments were fitted globally by the Hill equation with common values of the Hill coefficient and the value of MEK/MKP concentrations that gave a half maximal value of ERK phosphorylation. Plots were normalized by the upper baseline of the Hill equation.

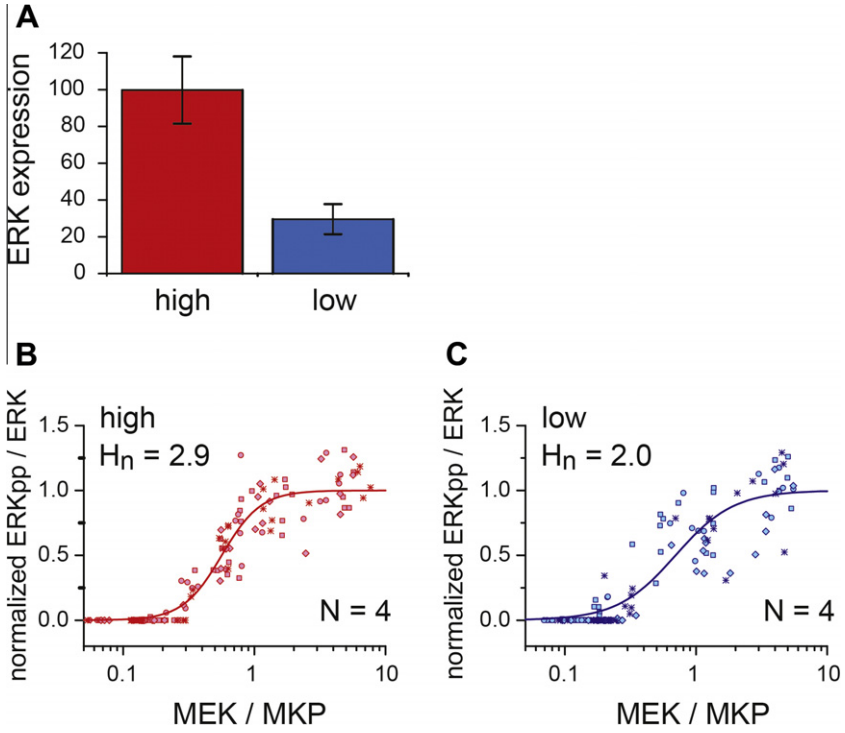

Fig. 2. Response characteristics of ERK activation as a function of MEK/MKP and ERK concentration. (A) ERK expression in the presence of 0.2% (high) or 0.066% (low) arabinose. The expression level was normalized to that in the presence of high arabinose. Error bars represent SD of 4 independent experiments. (B and C) Response curves of ERK activation as a function of the relative expression level of MEK and MKP in the presence of high (B) and low (C) arabinose. Changing the concentration of IPTG and aTc, 36 different culture conditions were examined as a single set, and four independent sets were carried out for either high and low arabinose concentration. The results of four different sets are shown in different symbols in each figure. The response curve was fitted by the Hill equation (line). H_n is Hill coefficient. In the Michaelis–Menten reaction model (Supplementary Tables 1 and 2), [MEK] and [MKP] are related parameters and the levels of ERKpp depend on [MEK]/[MKP] for each concentration of MEK and MKP.

2.6. Numerical analysis

We assumed two-step reactions both for ERK phosphorylation by MEK and dephosphorylation by MKP following Michaeles–Menten kinetics in the Marchevich model [26] (Fig. 1A). The parameters used for calculation are listed in Supplementary Table 1. Details of the reaction model are described in the legend of Supplementary Tables 1 and 2.

3. Results

3.1. Gene expressions of ERK, MEK and MKP

We first designed two expression vectors, one for ERK and another for MEK and MKP, and used these to transform *E. coli* cells (Fig. 1B, Supplementary Fig. 1). The expression levels of ERK, MEK, and MKP were independently regulated by placing their promoters under the control of three distinct inducers added to the culture media. Moreover, the expression levels of the individual proteins could be individually measured by monitoring the unique emission spectra of specific fluorescent proteins fused to the target proteins. In the ERK expression vector (pBAD), the expression of the ERK gene fused to that encoding the cyan fluorescent protein, Cerulean [18], was under the regulation of the arabinose-inducible araBAD promoter [19]. In order to control the experimental variables, an ERK mutant lacking kinase activity, K54A, was used [17]. In the tandem MEK/MKP expression vector (pACYC184), the expression of the MEK gene fused to that encoding the yellow fluorescent protein Venus [22] was under the regulation of the isopropyl-β-D-thiogalactopyranoside (IPTG)-inducible *lac* promoter [25]; and the expression of the MKP gene fused to that encoding the red fluorescent protein mCherry [23] was under the regulation of the anhydrotetracycline (aTc)-inducible *tet* promoter [25]. The MEK gene used in this study was a dual point/deletion mutant (S218/222E Δ32–51) which encodes a constitutively active kinase [20]. (MKP has no known regulation.)

In order to test our control of protein expression levels in this system, we monitored the fluorescence intensities of cells transformed with these plasmids in response to changing concentrations of inducers in the culture medium. The concentration of arabinose (for ERK) in the culture medium was kept constant while the concentrations of IPTG (for MEK) and aTc (for MKP) were varied systematically. As anticipated, MEK and MKP levels were induced in response to increasing IPTG and aTc concentrations, respectively, by a factor of 4 (MEK) or 45 (MKP), while the expression of ERK remained essentially constant (Fig. 1C–E). We observed positive correlations between the expression levels of the three proteins, which can possibly be attributed to the formation of stable complexes between these proteins which are conceivably more resistant to degradation.

3.2. ERK phosphorylation in E. coli cells

We next tested the function of the reconstructed ERK module by monitoring the phosphorylation status of ERK in the extract of *E. coli* cells co-transformed with the ERK and MEK/MKP vectors and treated with different combinations of inducers. As anticipated, ERK phosphorylation was detectable in cells co-transformed with ERK and MEK only after induction of MEK. Since tyrosine phosphorylation is characteristic of eukaryotes but not prokaryotes, we based our switch on a eukaryotic protein reaction system in order to minimize crosstalk between the reconstructed module and the host system. In order to verify this, we first used an anti-phospho-tyrosine antibody to assess the phosphorylation status

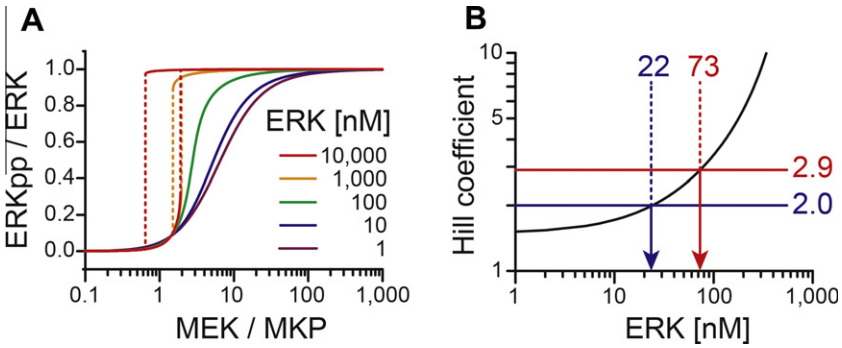

Fig. 3. Simulation of the change of the steepness of the switch. Response characteristics were calculated numerically assuming two-step Michaelis–Menten kinetics for both phosphorylations and dephosphorylations (Fig. 1A) (Section 2). (A) The response curve of ERK activation was calculated by changing the total concentration of ERK. In the Markevich model [26] used for calculation, a bistable response occurs above ~340 nM of ERK concentration (dotted lines). (B) Response curves as shown in (A) were fitted with Hill equation and the change of the best-fit value of the Hill coefficient was plotted against the ERK concentration. In the simulation, a reduction of the Hill coefficient from 2.9 to 2.0 was observed when the ERK concentration was reduced from 73 to 22 nM.

of endogenous proteins in *E. coli* cells co-expressing exogenous MEK and ERK. Only a single tyrosine-phosphorylated protein other than phospho-ERK was detectable in whole cell lysate of *E. coli* coexpressing MEK and ERK (Supplementary Fig. 2A) which, given that an inactive mutant of ERK was used, is likely attributable to MEK. While this tyrosine phospho-protein was detectable in cells without MEK induction, a significant amount of MEK was also detectable in the absence of the MEK inducer. Moreoever, while expression of MKP reversed ERK phosphorylation detected in the absence of the MEK inducer, it had no effect on the phosphorylation status of the endogenous *E. coli* tyrosine phospho-protein. We next used the anti-ERKpp antibody to examine whether ERK was phosphorylated by endogenous proteins in *E. coli* cells (Supplementary Fig. 2B). ERK phosphorylation was undetectable in cells without co-transformation of MEK, even in the presence of inducers for MEK and MKP, indicating that ERK was not phosphorylated by endogenous *E. coli* kinases. Taken together, our results indicate that the reconstructed module functions essentially independently of the host signaling systems.

3.3. Response characteristics of ERK module

We next used anti-ERKpp antibody Western blotting of whole cell lysates to evaluate the response characteristics of the ERK module in the presence of various expression levels of its regulatory components. Under a fixed concentration of arabinose (ERK inducer, 0.2%), dual-phosphorylation of ERK was measured in response to increasing concentration of IPTG (MEK inducer, 0–0.133 mM) and aTc (MKP inducer, 0–0.311 μg/ml). Theoretically, ERK dual-phosphorylation should be a function only of the ratio of MEK and MKP and not their absolute concentrations. Plotting normalized intensities of the anti-ERKpp antibody signal against the ratio of fluorescent intensities of Venus-MEK and mCherry-MKP (Fig. 2B), we found that dual-phosphorylation of ERK increased as a function of increasing MEK/MKP ratio in a sigmoidal manner with a midpoint at the fluorescence intensity ratio MEK/MKP = 0.6. The response curve was expressed by the Hill equation as a phenomenological fit. In the presence of 0.2% arabinose, the Hill coefficient (H_n) was 2.9. A H_n value >1 indicates that the module exhibits an ultrasensitive switch-like response.

Two possible mechanisms underlying the ultrasensitivity in our reconstructed module are (i) two-step reactions and (ii) zeroth-order ultrasensitivity [27]. Two-step reactions have an upper limit of $H_n = 2.0$ which is smaller than the observed value of 2.9 in the presence of 0.2% arabinose, indicating that a two-step reaction is not the sole mechanism underlying the ultrasensitivity of the module, and that zeroth-order ultrasensitivity may be involved. We performed numerical analysis of the reaction module in which Michaelis–Menten kinetics were assumed for the individual reaction steps (Fig. 1A, Supplementary Tables 1 and 2) [26]. Saturation of the kinase and/or the phosphatase reaction is the key assumption underlying zeroth-order ultrasensitivity (Fig. 3). After numerical calculations of the response curves at various ERK concentrations (Fig. 3A), the results were fitted by the Hill equation and H_n was plotted as a function of ERK concentration (Fig. 3B). The plot shows that H_n increases with the increase of ERK concentration by a mechanism identical to the increase of H_n with the decrease of the Michaelis constant (K_m), which has been reported as zeroth-order ultrasensitivity. (Actually, H_n is the function of K_m/[ERK].)

According to the prediction of the numerical analysis, we next attempted to control the steepness (H_n) of the reconstructed module by altering the ERK concentration. Reduction of the arabinose concentration to 0.066% resulted in a decrease of ERK expression by a factor of 0.29 (Fig. 2A). In this condition, the apparent H_n decreased to 2.0 (Fig. 2C). In the numerical analysis (Fig. 3B), the decrease of H_n from 2.9 to 2.0 is effected by the reduction of ERK concentration from 73 to 22 nM (a factor of 0.30). The experimental result is therefore roughly consistent with the theoretical prediction. Taken together, our results are consistent with a controllable, ultrasensitive protein-based switch-like module.

4. Discussions

Previous studies have reconstructed eukaryotic signal transduction reactions in the context of eukaryotic cells for the analysis of these reaction networks under controllable conditions [10]. Here we have demonstrated the reconstruction of a eukaryotic signaling pathway in a prokaryotic cell in order to permit regulation of the reconstructed module independent of the host cell system. Reconstructions of eukaryotic reactions in prokaryotic cells expand the design parameters of artificial biological circuits to encompass both transcription and posttranslational components. In addition, we have demonstrated that a protein switch-like module can be regulated in response to a single element, and does not require protein modification, localization, or addition of regulatory elements. This type of regulation expands the potential application of artificial biological circuits to the modulation of cell behavior.

Acknowledgments

The authors thank Rie Nakazawa and Yasue Ichikawa for DNA sequencing and Hiromi Sato for technical assistance.

Appendix A. Supplementary data

Supplementary data associated with this article can be found, in the online version, at http://dx.doi.org/10.1016/j.bbrc.2012.04.071.

References

[1] S. Mukherji, A. van Oudenaarden, Synthetic biology: understanding biological design from synthetic circuits, Nature Review Genetics 10 (2009) 859–871.
[2] T.K. Lu, A.S. Khalil, J.J. Collins, Next-generation synthetic gene networks, Nature Biotechnology 27 (2009) 1139–1150.
[3] P.E.M. Purnick, R. Weiss, The second wave of synthetic biology: from modules to systems, Nature Review Molecular Cell Biology 10 (2009) 410–422.
[4] D. Sprinzak, M.B. Elowitz, Reconstruction of genetic circuits, Nature 438 (2005) 443–448.
[5] N. Nandagopal, M.B. Elowitz, Synthetic biology: integrated gene circuits, Science 333 (2011) 1244–1248.
[6] W.A. Lim, Designing customized cell signalling circuits, Nature Review Molecular Cell Biology 11 (2010) 393–403.
[7] B.J. Yeh, R.J. Rutigliano, A. Deb, D. Bar-Sagi, W.A. Lim, Rewiring cellular morphology pathways with synthetic guanine nucleotide exchange factors, Nature 447 (2007) 596–600.
[8] S.-H. Park, A. Zarrinpar, W.A. Lim, Rewiring MAP kinase pathways using alternative scaffold assembly mechanisms, Science 299 (2003) 1061–1064.
[9] C.J. Bashor, N.C. Helman, S. Yan, W.A. Lim, Using engineered scaffold interactions to reshape MAP kinase pathway signaling dynamics, Science 319 (2008) 1539–1543.
[10] E.C. O'Shaughnessy, S. Palani, J.J. Collins, C.A. Sarkar, Tunable signal processing in synthetic MAP kinase cascades, Cell 144 (2011) 119–131.
[11] A. Goldbeter, D.E. Koshland, An amplified sensitivity arising from covalent modification in biological systems, Proceedings of the National Academy of Sciences of the United States of America 78 (1981) 6840–6844.
[12] W. Kolch, Meaningful relationships: the regulation of the Ras/Raf/MEK/ERK pathway by protein interactions, Biochemical Journal 351 (Pt 2) (2000) 289–305.
[13] C.J. Marshall, Specificity of receptor tyrosine kinase signaling: transient versus sustained extracellular signal-regulated kinase activation, Cell 80 (1995) 179–185.
[14] W.R. Burack, T.W. Sturgill, The activating dual phosphorylation of MAPK by MEK is nonprocessive, Biochemistry 36 (1997) 5929–5933.
[15] J.E. Ferrell, R.R. Bhatt, Mechanistic studies of the dual phosphorylation of mitogen-activated protein kinase, The Journal of Biological Chemistry 272 (1997) 19008–19016.
[16] Y. Zhao, Z.Y. Zhang, The mechanism of dephosphorylation of extracellular signal-regulated kinase 2 by mitogen-activated protein kinase phosphatase 3, The Journal of Biological Chemistry 276 (2001) 32382–32391.
[17] M.J. Robinson, P.C. Harkins, J. Zhang, R. Baer, J.W. Haycock, M.H. Cobb, E.J. Goldsmith, Mutation of position 52 in ERK2 creates a nonproductive binding mode for adenosine 5′-triphosphate, Biochemistry 35 (1996) 5641–5646.
[18] M.A. Rizzo, G.H. Springer, B. Granada, D.W. Piston, An improved cyan fluorescent protein variant useful for FRET, Nature Biotechnology 22 (2004) 445–449.
[19] L.M. Guzman, D. Belin, M.J. Carson, J. Beckwith, Tight regulation, modulation, and high-level expression by vectors containing the arabinose P_{BAD} promoter, Journal of Bacteriology 177 (1995) 4121–4130.
[20] S.J. Mansour, W.T. Matten, A.S. Hermann, J.M. Candia, S. Rong, K. Fukasawa, G.F. Vande Woude, N.G. Ahn, Transformation of mammalian cells by constitutively active MAP kinase kinase, Science 265 (1994) 966–970.
[21] T. Furukawa, T. Yatsuoka, E.M. Youssef, T. Abe, T. Yokoyama, S. Fukushige, E. Soeda, M. Hoshi, Y. Hayashi, M. Sunamura, M. Kobari, A. Horii, Genomic analysis of DUSP6, a dual specificity MAP kinase phosphatase, in pancreatic cancer, Cytogenetics and Cell Genetics 82 (1998) 156–159.
[22] T. Nagai, K. Ibata, E.S. Park, M. Kubota, K. Mikoshiba, A. Miyawaki, A variant of yellow fluorescent protein with fast and efficient maturation for cell-biological applications, Nature Biotechnology 20 (2002) 87–90.
[23] N.C. Shaner, R.E. Campbell, P.A. Steinbach, B.N. Giepmans, A.E. Palmer, R.Y. Tsien, Improved monomeric red, orange and yellow fluorescent proteins derived from *Discosoma* sp. red fluorescent protein, Nature Biotechnology 22 (2004) 1567–1572.
[24] J. Shine, L. Dalgarno, Determinant of cistron specificity in bacterial ribosomes, Nature 254 (1975) 34–38.
[25] R. Lutz, H. Bujard, Independent and tight regulation of transcriptional units in *Escherichia coli* via the LacR/O, the TetR/O and AraC/I_1-I_2 regulatory elements, Nucleic Acids Research 25 (1997) 1203–1210.
[26] N.I. Markevich, J.B. Hoek, B.N. Kholodenko, Signaling switches and bistability arising from multisite phosphorylation in protein kinase cascades, The Journal of Cell Biology 164 (2004) 353–359.
[27] J.E. Ferrell, Tripping the switch fantastic: how a protein kinase cascade can convert graded inputs into switch-like outputs, Trends in Biochemical Sciences 21 (1996) 460–466.